ACS Catalysis

Research Article

pubs.acs.org/acscatalysis

Boron Nitride: A Support for Highly Active Heteropolyacids in the Methanol-to-DME Reaction

Josefine Schnee, Adrien Eggermont, and Eric M. Gaigneaux*

Institute of Condensed Matter and Nanosciences (IMCN) − MOlecules Solids and reactiviTy (MOST), Université catholique de Louvain (UCL), Place Louis Pasteur 1, box L4.01.09, 1348 Louvain-la-Neuve, Belgium

Supporting Information

ABSTRACT: Due to its superacidity and ability of its bulk to react following a pseudoliquid mechanism, the Keggin $H_3PW_{12}O_{40}$ heteropolyacid attracts more and more attention as a catalyst for the gas phase methanol-to-DME reaction. However, in its pure state, $H_3PW_{12}O_{40}$ has a very low surface area (typically 5−10 m^2/g), which limits the accessibility of its inner protons due to diffusional constraints and explains why teams investigate $H_3PW_{12}O_{40}$ in its supported form. In the present work, we highlight the interest of using hexagonal boron nitride (BN) as a support. We show that, in contrast to commonly used supports such as TiO_2, BN is able to increase the accessibility of $H_3PW_{12}O_{40}$'s acid sites (i.e., stabilizing small enough crystallites) while preserving their strong acidity (i.e., not interacting too much with the Keggin units). At low loadings (typically around 16% of one ideal Keggin monolayer), BN leads $H_3PW_{12}O_{40}$ to reach an almost 2 times higher methanol conversion than obtained with the adequately activated pure bulk sample, and an almost 10 times higher conversion than an optimized TiO_2-supported $H_3PW_{12}O_{40}$ catalyst. At higher $H_3PW_{12}O_{40}$ loadings, the BN-supported catalysts are still much more active than the optimized TiO_2-supported one, but less active than the pure bulk-activated $H_3PW_{12}O_{40}$, which we attribute to the partial intercalation of $H_3PW_{12}O_{40}$ within the interlayers of BN.

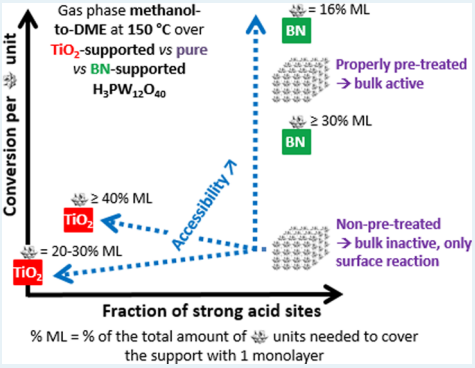

KEYWORDS: *Keggin heteropolyacid, hexagonal boron nitride, methanol dehydration, dimethyl ether, supported catalysts, titanium dioxide*

1. INTRODUCTION

Heteropolyacids (HPAs) are metal−oxygen clusters that are nowadays widely used in acid catalysis. Indeed, thanks to their exceptionally high Brönsted acidity, they generally allow operating chemical reactions under milder conditions than required by conventional acid catalysts.[1] The most easily available HPAs, namely the Keggin ones, have the general formula $H_nXM_{12}O_{40}$. They contain $[XM_{12}O_{40}]^{n-}$ heteropolyanions stabilized by n acidic protons, with X being the heteroatom (often P^{5+}, Si^{4+}) and M being the addenda atom (transition metal, typically Mo^{6+}, W^{6+}).[2] In particular, a reaction for which Keggin HPAs currently attract more and more attention as catalysts is the gas phase dehydration of methanol to dimethyl ether (DME).[3,4] The latter is indeed one of the most promising alternative fuels for the future, as it has a particularly low climate impact (being biodegradable, noncorrosive, and nontoxic and burning without emission of particulates or nitrous oxides).[5,6]

As pure Keggin HPAs have a very low specific surface area (typically 5−10 m^2/g), the strategy that is generally followed with the intention of exploiting to the best their catalytic potential is to disperse them on a support which does not alter their Keggin structure. A typical support used in this purpose is TiO_2.[3,4,7,8] Indeed, in the methanol-to-DME reaction, $H_3PW_{12}O_{40}$ and $H_4SiW_{12}O_{40}$ (the two most acidic and most widely used Keggin HPAs) have been shown to exhibit higher activities when being supported on TiO_2 than when being used pure.[3,4] However, what has not been considered up to this point in the latter comparison is that methanol, as a polar molecule, is actually able to react both at the surface and within the bulk of the pure HPAs if the latter have been pretreated adequately. Indeed, unprecedented, we have recently shown[9] that the following pretreatment procedure allows activating the bulk of a Keggin HPA so that it contributes converting methanol additionally to the surface: dehydrating the HPA at about 300 °C under nitrogen, then cooling it down to 25 °C and exposing it to methanol, and only then heating it to the reaction temperature. The exposure to methanol at 25 °C is the crucial step that allows the bulk penetration, and the dehydration is required for methanol to reach the HPA's acidic protons once it has penetrated the bulk. Such a procedure has never been applied in the reported studies comparing supported and pure HPAs.

In the present work, we investigate for the first time the performance of $H_3PW_{12}O_{40}$ in the methanol-to-DME reaction when being supported on hexagonal boron nitride (BN), a

Received: March 13, 2017
Revised: April 14, 2017
Published: May 4, 2017

DOI: 10.1021/acscatal.7b00808
ACS Catal. 2017, 7, 4011−4017

layered material with a graphite-like structure in which planar networks of BN hexagons are regularly stacked,[10] namely a support which is much less conventional for HPAs than TiO_2. By using the pure $H_3PW_{12}O_{40}$ in its most active state (namely, with its bulk being active additionally to its surface) and TiO_2-supported $H_3PW_{12}O_{40}$ as references, we demonstrate that BN is an excellent support for $H_3PW_{12}O_{40}$ in the methanol-to-DME reaction, far more suitable than conventional supports such as TiO_2.

2. EXPERIMENTAL SECTION

2.1. Materials—Catalyst Preparation. $H_3PW_{12}O_{40}$ (hereafter, HPW12) was purchased from Sigma-Aldrich in the form of $H_3PW_{12}O_{40}{\cdot}xH_2O$ (reagent grade). It was supported on BN (hexagonal, Sigma-Aldrich, ≈ 1 μm, 98%, 19 m^2/g) by wet impregnation at room temperature. A series of reference samples supported on TiO_2 (Degussa P25, 20% rutile −80% anatase, 50 m^2/g) was also prepared by exactly the same method. Precisely, the appropriate amounts of HPW12 (corresponding to the nominal loadings reported in Table S1 in the Supporting Information) were dissolved in ethanol (AnalaR NORMAPUR, >99,8%) and then added dropwise to 1 g of support dispersed also in ethanol. The resulting mixtures were stirred for 2 h, before the solvent was evaporated in a rotary evaporator at 40 °C. Finally, the samples were dried overnight in a vacuum oven (<5000 Pa) at room temperature. Their real HPW12 loadings were determined through inductively coupled plasma atomic emission spectrometry (ICP-AES) with an ICAP 6500 Thermo Scientific and are expressed hereafter in "% ML," namely as percentages of the total amount of Keggin units theoretically required to cover the supports with one ideal monolayer (abbreviated here to "ML"). So, all results are discussed here with respect to the real HPW12 loadings (ranging from 16 to 92% ML on BN and from 21 to 86% ML on TiO_2), not to the nominal ones (both being however in good agreement, as shown by Table S1). Moreover, the fact that the loadings are expressed in % ML implies that the dispersion of HPW12 from one support to the other is independent of their respective specific surface area. The unsupported HPW12 sample used as a reference (named "pure HPW12" hereafter) was obtained through exactly the same procedure as described above for the impregnation, but without introduction of support. Notice that both supports are exclusively macroporous; they do not contain micro- or mesopores (see the N_2 physisorption isotherms on Figure S1 in the Supporting Information, measured with a Micromeritics Tristar Surface Area and Porosity Analyzer after having degassed the samples overnight at 150 °C under a vacuum of about 80 mTorr).

2.2. Physico-chemical Characterization. Fourier transform infrared (FT-IR) spectra were recorded in transmission mode using an IFS55 Equinox spectrometer (Bruker) equipped with a DTGS detector. A total of 100 scans per spectrum were recorded between 400 and 4000 cm^{-1} with a resolution of 4 cm^{-1}. Pellets were prepared after dilution of the samples in KBr (Janssens Chimica 99%) by a 100 weight factor.

Powder X-ray diffraction (XRD) patterns were measured at room temperature with a Kristalloflex Siemens D5000 diffractometer using copper K_α radiation (λ = 0.15418 nm) and equipped with a scintillation detector (the X-ray source working with a tension of 40 kV and a current of 40 mA).

X-ray photoelectron spectroscopy (XPS) was performed with a SSX 100/206 spectrometer from Surface Science Instruments (USA) equipped with a monochromatized and microfocused Al X-ray source (powered with 20 mA and 10 kV). The pressure within the analysis chamber was about 10^{-6} Pa. The angle between the normal to the surface and the axis of the input lens of the analyzer was 55°. The zone analyzed was about 1.4 mm^2, and the pass energy was set at 150 eV for the general spectra and at 50 eV for the elementary spectra. An electron gun set at 8 eV and a nickel grid placed 3 mm above the surface of the samples were used to stabilize the charge. The following sequence of spectra was recorded: general spectrum, C 1s, O 1s, N 1s (as the support was BN), B 1s (as the support was BN), Ti 2p (as the support was TiO_2), W 4d, P 2p, and again C 1s to check the stability of the charge compensation as a function of time and the absence of sample degradation. The C-(C,H) component of the C 1s peak of carbon was fixed at 284.8 eV to set the binding energy scale. When required, spectra were decomposed with the CasaXPS program (Casa Software Ltd., UK) with a Gaussian/Lorentzian product function after subtraction of a nonlinear baseline. For the quantification of the elements, the sensitivity factors and acquisition parameters provided by the manufacturer were used.

NH_3 adsorption and subsequent temperature-programmed desorption (NH_3-TPD) were performed in a Hiden CATLAB-PCS combined microreactor and mass spectrometer (MS) system (the MS being equipped with a quadrupole). Experiments were performed according to the following three steps: (1) stabilization of a flow of pure He (30 mL/min) at 50 °C for 25 min in order to check the sensitivity factor of He and therewith to determine that of NH_3 during the later TPD (through the previously calibrated He/NH_3 sensitivity factors ratio) and subsequent heating to 150 °C (still under 30 mL/min of pure He); (2) adsorption of NH_3 at 150 °C for 1.5 h from a 95:5 He/NH_3 flow (25 mL/min) mixed with a flow of pure He (5 mL/min); (3) flush at 150 °C under pure He (30 mL/min) for 2.5 h in order to eliminate physisorbed NH_3 and subsequent TPD from 150 to 650 °C (10 °C/min, still under 30 mL/min of pure He) in order to desorb chemisorbed NH_3 (of which the MS response reflects the number of acids sites within the samples, and the desorption temperature reflects the latter acid sites' strength). It was checked that no side compounds as N_2 or NO_x were desorbed.

N_2 physisorption was performed only for the pure supports (as described in section 2.1), not for the catalysts. Indeed, being apolar, N_2 does not penetrate into the bulk of HPW12 (in contrast to NH_3).[11] As a consequence, specific surface area values measured through N_2 physisorption may not be correlated to catalytic activity data in the reaction of a polar molecule such as methanol, which is susceptible to penetration/reaction in HPW12's bulk (certainly when our bulk activation pretreatment explained in section 1 is applied).

2.3. Catalytic Tests. Catalytic tests in the methanol-to-DME reaction were launched by introducing a given amount of catalyst powder sieved within 100−200 μm into a tubular reactor (fixed bed), by placing the latter under a 30 mL/min inflow of nitrogen (Praxair 5.0) saturated with 10 vol % of methanol (Sigma-Aldrich, anhydrous, 99.8%) at atmospheric pressure, and finally by heating the whole system from room temperature to a reaction temperature of 150 °C (the latter procedure having been applied to all catalysts including the pure HPW12, but with the latter having additionally been tested after our bulk activation pretreatment described in section 1). As all tests were performed with the same catalyst bed height in order to maintain a constant contact time (0.023

DOI: 10.1021/acscatal.7b00808
ACS Catal. 2017, 7, 4011−4017

min), the amount of catalyst introduced was different depending on the HPW12 loading (the reason why the results are discussed in section 3 per gram of catalyst and per gram of HPW12). Regarding the pure HPW12, it was diluted with glass beads also sieved within 100−200 μm (and previously checked to be inactive in the reaction conditions used here). In all tests, the outlet gas flow was analyzed every 5.5 min by an Interscience compact gas chromatograph equipped with a Rtx-1 1.5 μm column (15 m × 0.32 mm) followed by a flame ionization detector. DME was always the only product of methanol conversion detected (selectivity of 100%).

3. RESULTS AND DISCUSSION

3.1. Physico-chemical Characterization. The BN-supported catalysts show the same FT-IR bands as the pure HPW12 (Figure 1), indicating that the latter's Keggin structure

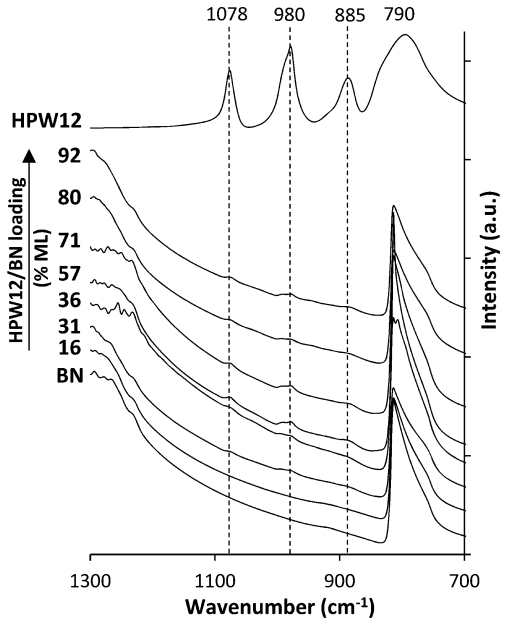

Figure 1. FT-IR spectra (transmission mode) of the BN-supported catalysts (HPW12 loadings from 20 to 90% ML), as well as of pure BN and pure HPW12.

was maintained upon impregnation (exactly as for the equivalent TiO_2-supported catalysts with the same nominal/very close real loadings in % ML, see Figure S2 in the Supporting Information). The latter bands, positioned at 1080, 980, 885, and 790 cm^{-1}, are respectively due to P−O_a−W, W═O_d, W−O_b−W, and W−O_c−W vibrations. The band at 800 cm^{-1} in Figure 1 is due to intersheet vibrations of sp^2 B−N bonds, whereas the one starting to emerge at 1100 cm^{-1} is due to intrasheet vibrations of sp^2 B−N bonds.[12] On the full spectrum of pure BN shown in Figure S3b in the Supporting Information, only a slight O−H band is observed around 3400 cm^{-1}, having a considerably lower relative intensity (as compared to BN's main bands) than that observed on the spectrum of pure TiO_2 (as compared to TiO_2's main bands, Figure S3a). This reflects that BN retains less physisorbed water than TiO_2, which agrees with the water contact angles reported in the literature (35 and 86° respectively for TiO_2 and BN)[13−15] and indicating that BN is less hydrophilic than TiO_2. The latter property has to be kept in mind here, as Keggin units are highly polar[16] and might thus be less tempted to disperse over BN than over TiO_2.

Indeed, according to Figure 2, showing the surface atomic ratio of W over the constitutive elements of BN (Figure 2a)

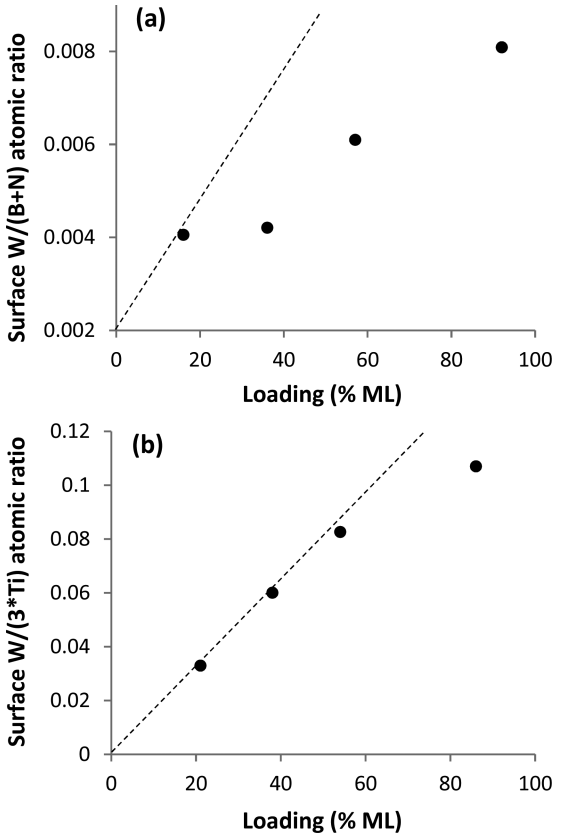

Figure 2. XPS-measured surface atomic ratios W/(B + N) (a) and W/(3 × Ti) (b) respectively of the BN-supported and TiO_2-supported catalysts as a function of the HPW12 loading (% ML). The factor 3 in the denominator of W/(3 × Ti) accounts for the O atoms of TiO_2. The latter cannot be distinguished from the O atoms of HPW12 but represent two of the three constitutive atoms of TiO_2 and therefore need to be taken into account to allow a proper comparison to the BN-supported catalysts.

and of TiO_2 (Figure 2b) as a function of the HPW12 loading (% ML), HPW12's Keggin units interact differently with BN than with TiO_2. Instead of continuously increasing from 16 to 92% ML as the W/(3 × Ti) ratio of the TiO_2-supported catalysts does from 21 to 86% ML (Figure 2b), the W/(B + N) ratio first stays constant from 16 to 36% ML, and only then it does increase (by almost the same factor from 36 to 92% ML as the W/(3 × Ti) ratio on Figure 2b from 38 to 86% ML, namely by 2 vs 1.83, respectively). This suggests that, unlike what occurs on TiO_2 (essentially a dispersion as an ideal monolayer of Keggin units over the whole loading range), the Keggin units start to disperse on BN only above 36% ML. Below the latter threshold, they only stack on each other (either starting from the surface of BN, or forming independent aggregates). Furthermore, even above 36% ML, the Keggin units still disperse to a lower extent than on TiO_2, as the W/(B + N) ratios on Figure 2a are always drastically lower than the W/(3 × Ti) ones on Figure 2b (e.g., at about 40% ML, W/(B + N) = 0.004 vs W/(3 × Ti) = 0.06). So, all over the here explored loading range, Keggin units interact to a significant extent with

DOI: 10.1021/acscatal.7b00808
ACS Catal. 2017, 7, 4011−4017

each other instead of interacting with BN, with however a certain fraction of them starting to disperse on BN above 36% ML (the aim here being not to precisely evaluate the latter fraction).

On the XRD patterns, up to 36% ML, only the diffraction signal of BN is observed (see the latter's pattern on Figure 3).

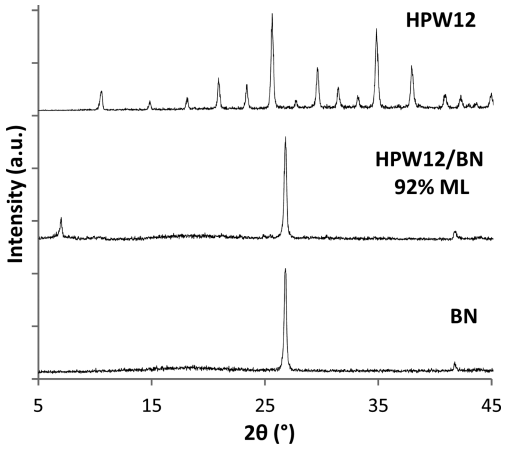

Figure 3. XRD patterns of the BN-supported catalyst with 90% ML of HPW12, as well as of pure BN and pure HPW12.

Then, above 36% ML, an additional peak appears at $2\theta = 6.9°$ (see on Figure 3 the pattern of the catalyst with 92% ML, which is representative of all catalysts with loadings higher than 36% ML). This peak can only have three origins: (1) HPW12 crystals having become large enough to be detected, (2) HPW12 crystals being still too small to be detected but having dispersed on BN following a precise intercrystal repeated distance, or (3) Keggin units having locally penetrated/enlarged the interlayers of BN (and so caused the shift of the main diffraction peak of the concerned regions of BN from $2\theta = 26.7°$ to lower angles). The first possibility can be excluded as the diffraction pattern of pure/crystalline HPW12 does not contain any peak at 6.9° (see the latter's pattern also on Figure 3). The second possibility is conceivable only with HPW12 crystals being broad as one single Keggin unit (so being made of one single column of Keggin units stacked on each other, and thus actually corresponding to "periodic aggregates" instead of "crystals"). Indeed, with a broadness of 1 nm per Keggin unit,[17] a crystal having a broadness of minimum 2 Keggin units is alone broader than the repeated distance corresponding to the diffraction peak at 6.9°, namely 1.33 nm. Such a crystal could thus not be repeated following the latter distance. However, even in the case of HPW12 aggregates broad as one single Keggin unit, the question remains why the interaggregate distance would be so well-defined instead of aleatory. The third possibility is more realistic insofar as a shift of BN's main diffraction peak from 26.7 to 6.9° would reflect an increase of about 1 nm of its interlayer distance, namely precisely the diameter of a Keggin unit. Moreover, there are studies in the literature that report that the intercalation of Brönsted acids in between the layers of hexagonal BN is indeed possible and easy (simple drying of BN in the acids, as done here). This has been demonstrated for H_2SO_4, H_3PO_4, and $HClO_4$, and hydrogen bonds of the latter acids to the basic N atoms of the BN sheets have been shown to drive the intercalation process.[18] To our knowledge, an HPW12-intercalated BN is not yet explicitly reported in the literature. There is one study[19] in which the authors claim to have confined HPW12 within BN (for liquid phase oxidative desulfurization), but the BN used (and synthesized by the authors) is microporous (in contrast to our commercial one), and it is not clear whether HPW12's Keggin units are confined within the micropores (having indeed space for one or two units) and/or in between the BN sheets. Actually, the XRD patterns reported in ref 19 have been measured only down to $2\theta = 10°$ (and they show the characteristic peaks of crystalline HPW12, indicating that a significant part of the Keggin units is actually not directly in contact with BN). Nevertheless, the interactions between BN sheets being weak (of electrostatic nature),[18] the intercalation of Keggin units, even if they are broader than the acids used in ref 18, is truly conceivable and should be retained here as the most likely explanation for the appearance of the diffraction peak at 6.9° in Figure 3 (which does still not exclude the presence of periodic aggregates of Keggin units at the surface of BN arranged following an aleatory interaggregate distance and thus not giving rise to any diffraction peak). Notice that, based on the latter explanation, the increasing surface W/(B + N) ratio above 36% ML on Figure 2a should actually be interpreted as reflecting the dispersion of Keggin units within the interlayers of BN crystals instead of simply at their outer surface. In any case, the fact that the concerned BN-supported catalysts show a new diffraction peak that is not part of the patterns of pure BN and pure HPW12, and additionally that do not show any of the characteristic diffraction peaks of pure HPW12, demonstrates that the Keggin units interact with BN instead of forming independent aggregates.

As analyzed by NH_3-TPD, the BN-supported catalysts with HPW12 loadings between 16 and 36% ML do not show any desorption signal over the whole analyzed temperature range (150 to 700 °C), exactly as the pure BN (Figure S4 in the Supporting Information). This is attributed to the very low HPW12 weight fractions contained in these catalysts (e.g., 1.5 and 3.4 wt %, respectively, in the 16 and 36% ML catalysts), and not to the absence of acid sites (except in the case of pure BN). However, introducing a higher mass of the concerned catalysts into the TPD setup was not relevant, as doing so leads to temperature inhomogeneities within the sample beds and to pressure drop issues. Figure 4 shows the NH_3-TPD profiles of the BN-supported catalysts with HPW12 loadings between 57 and 92% ML. These profiles reflect the presence of exclusively strong acid sites (characterized by an NH_3-desorption signal above 500 °C[20,21]), unlike the profiles of the equivalent TiO_2-supported catalysts (Figure 5) which reflect the presence of quasi-exclusively medium acid sites (characterized by an NH_3-desorption signal from 300 to 500 °C,[20,21] each signal attributed to HPW12 being marked by a star on Figure 5). Actually, the BN-supported catalysts with loadings from 57 to 80% ML show their NH_3-desorption maximum at an even higher temperature than the pure HPW12 (630 and 610 °C, respectively, for the 57−71 and 80% ML BN-supported catalysts, vs 600 °C for the pure HPW12 as well as for the 92% ML BN-supported catalyst). This reflects that, in the loading range from 57 to 80% ML, BN stabilizes the Keggin units from thermal decomposition[1] into WO_3 and P_2O_5 and so shifts the release of NH_3 retained in between them to higher temperatures (the NH_3-desorption maximum of pure HPW12 at 600 °C corresponding actually to the thermal decomposition of the $(NH_4)_3PW_{12}O_{40}$ ammonium salt formed along with the chemisorption of NH_3 onto the bulk protons of crystalline

DOI: 10.1021/acscatal.7b00808
ACS Catal. 2017, 7, 4011−4017

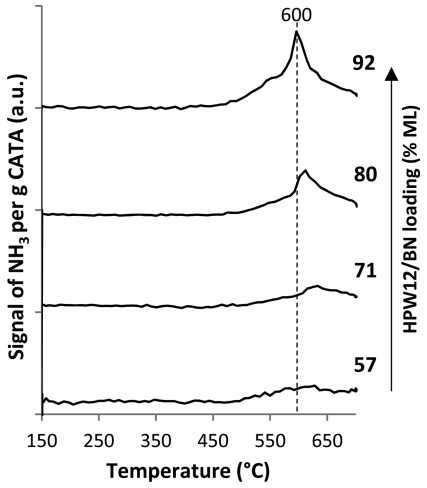

Figure 4. NH_3-TPD profiles of the BN-supported catalysts with HPW12 loadings between 60 and 90% ML (after NH_3 adsorption at 150 °C, and normalization per gram of catalyst introduced).

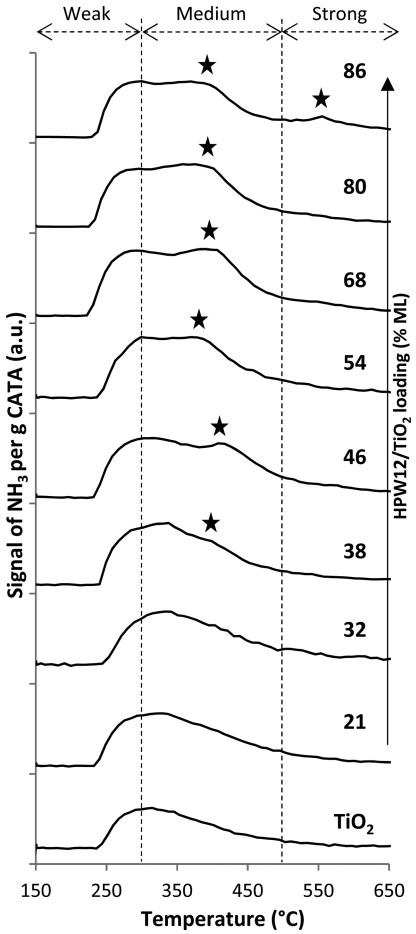

Figure 5. NH_3-TPD profiles of the TiO_2-supported catalysts with HPW12 loadings between 20 and 90% ML, as well as of pure TiO_2 (after NH_3 adsorption at 150 °C, and normalization per gram of catalyst introduced).

HPW12 aggregates[20]). Whatever the reason for this stabilization from 57 to 80% ML (not further studied here), it can be stated that, in contrast to TiO_2, BN does not induce a significant weakening of HPW12's acid sites in the loading range from 57 to 92% ML (all detected sites staying at least as strong as in the pure HPW12, whereas on TiO_2, protons are shared[3] with the support and thus are less available to form an integer ammonium salt stable up to 600 °C, which means, in other words, that they are less acidic, leading to less strongly bonded NH_3). Although the NH_3-TPD profiles of the BN-supported catalysts with HPW12 loadings lower than 57% ML cannot be exploited, it can be confidently assumed that the above enunciated statement for 57−92% ML loadings is also valid for lower loadings. Indeed, as reflected by the XPS results on Figure 2a, the closest HPW12−BN interaction (close in the sense that the Keggin units' dispersion over BN increases with the HPW12 loading) occurs at loadings higher than 36% ML. That is why, if weaker acid sites do not appear in the highest HPW12-BN interaction state, they are unlikely to appear in the lowest HPW12-BN interaction state (low in the sense that the Keggin units tend to stack on each other instead of dispersing over BN), at least not as representing a significant fraction of the total number of acid sites.

3.2. Catalytic Performance. Figures 6, 7, and 8 show the conversion of methanol (mean value over 6 h of reaction

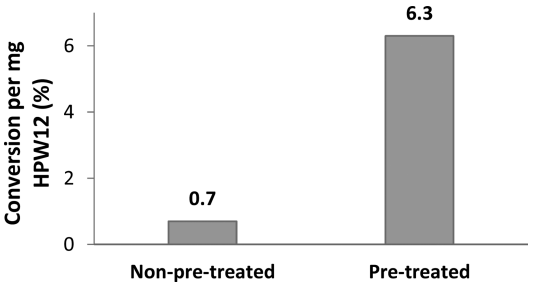

Figure 6. Conversion of methanol at 150 °C over pure HPW12 (normalized per milligram of HPW12 introduced) with and without pretreatment (1 h at 350 °C under pure nitrogen, followed by 10 min at 25 °C under nitrogen saturated with 10 vol % of methanol—namely the reaction flow—followed by heating from 25 °C to reaction temperature 150 °C).

throughout which no deactivation occurred) obtained at 150 °C respectively with the pure HPW12, the BN-supported catalysts, and the TiO_2-supported catalysts (as a function of the HPW12 loading in % ML in the case of the supported catalysts and depending on whether the bulk activation procedure described in section 1 has been applied or not in the case of pure HPW12). In Figures 7a and 8a, the conversion is normalized per milligram of each catalyst, while in Figures 6, 7b, and 8b, it is normalized per milligram of HPW12 contained in each catalyst (the weight used of each catalyst being given in Table S1, and the methanol conversion rates in moles of methanol/milligram of catalyst/hour being provided in Table S2). Indeed, as explained in section 2, all catalysts have been tested with the same methanol−catalyst contact time (same catalyst bed height and same methanol flow rate). As a consequence, from one catalyst to the other, the weight of HPW12 introduced was different (depending on the latter's loading). Normalizing as described above makes sense insofar as the raw conversions (not shown) are all below the equilibrium conversion (namely below 85%, as measured in a separate experiment, not shown). Notice that the conversion per milligram of pure HPW12 in Figure 6 increases as much as from 0.7% without pretreatment to 6.3% with bulk activation pretreatment. The latter pretreatment is thus really crucial in order to have a proper reference for the supported catalysts.

DOI: 10.1021/acscatal.7b00808
ACS Catal. 2017, 7, 4011−4017

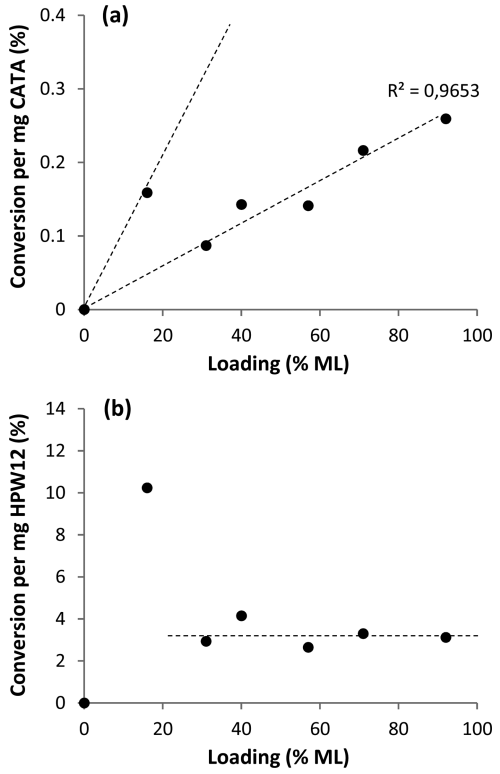

Figure 7. Conversion of methanol at 150 °C over the BN-supported catalysts as a function of the HPW12 loading (% ML), normalized (a) per milligram of each catalyst and (b) per milligram of HPW12 contained within each catalyst.

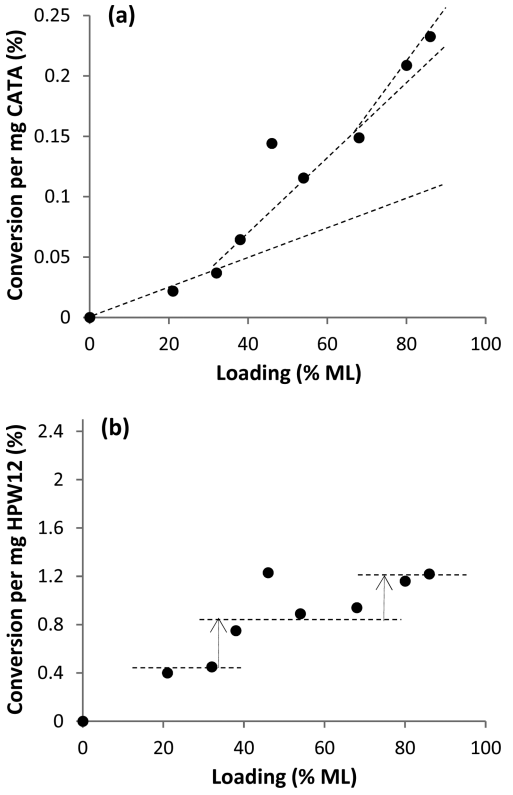

Figure 8. Conversion of methanol at 150 °C over the TiO_2-supported catalysts as a function of the HPW12 loading (a) per milligram of each catalyst and (b) per milligram of HPW12 within each catalyst. As following the dotted lines, exact agreement with the NH_3-TPD results in the following: (a) the slope of the conversion vs loading line increases every time the acid strength increases together with the number of acid sites, reflected in (b) by a jump (marked by an arrow) of the conversion per milligram of HPW12 from one dotted line (along which only the number of Keggin units/acid sites increases, not their activity/strength) to another higher one (as making exception of the value at 46% ML).

The conversion per milligram of BN-supported catalyst (Figure 7a) first increases from 0% at 0% ML of HPW12 (pure BN) to 0.16% at 16% ML of HPW12. Then, instead of further increasing along the line passing through the first two values, it drops to 0.09% at 31% ML. From then, it increases linearly with the HPW12 loading (as indicated by the linear regression coefficient R^2 being higher than 0.95), which reflects that the increase of number of acid sites (see the NH_3-TPD profiles on Figure 4) along with the increase of HPW12 loading occurs without a significant loss of accessibility/activity per Keggin unit. Indeed, as normalized per milligram of HPW12 (Figure 7b), the conversion is almost constant from 31 to 92% ML (except at 36% ML, at which it slightly increases). In other words, from 31 to 92% ML, increasing the HPW12 loading on BN does not lead to the formation of increasingly large diffusion-limited aggregates of Keggin units (as this would make the conversion per milligram of HPW12 progressively decrease). If aggregates are formed, either their dimensions are below a threshold above which significant internal diffusion limitations appear, or methanol does not penetrate/react in their bulk (this could not be checked by applying the bulk activation procedure explained in section 1 for pure HPW12, as doing so would segregate HPW12 from BN due to the heating step). In any case, the catalysts with 31 to 92% ML of HPW12 (showing acid sites as strong as the ones of pure HPW12, see Figure 4) have a lower conversion per milligram of HPW12 than the pure pretreated HPW12 (Figure 6) of which the bulk has been rendered accessible to methanol (though with diffusion limitations, as evidenced by following the conversion as a function of the flow rate, not shown). Indeed, additional to the possibility that methanol potentially reacts at the only surface of small HPW12 aggregates at the surface of BN, one has to remember that the XRD patterns on Figure 3 suggest that Keggin units have penetrated into the interlayers of BN. These interlayers might be less easy to penetrate by methanol under reaction conditions than the bulk of the pure pretreated HPW12. There is however one catalyst that shows a higher conversion per milligram of HPW12 than the pure pretreated HPW12: the one with 16% ML of HPW12 (10.2 vs 6.3% of conversion/milligram of HPW12, respectively). At such a low HPW12 loading, it is difficult to state whether the Keggin units would already be within BN's interlayers or not (the XRD pattern does not show the peak at 6.9°, but this could also be due to the very low fraction of BN concerned with the interlayer penetration). However, it is reasonable to assume that, kinetically, the penetration of BN's interlayers is less favored at low HPW12 loadings than at high ones. In any case, the BN-supported catalyst with 16% ML of HPW12 obviously has Keggin units more accessible than all the other BN-supported catalysts with higher HPW12 loadings and than the pure, although bulk-activated, HPW12 (its higher performance per milligram of HPW12 not being justifiable by a higher acid strength, as the Keggin units within the catalysts with higher HPW12 loadings and within the pure HPW12 have already the highest possible acid strength).

DOI: 10.1021/acscatal.7b00808
ACS Catal. 2017, 7, 4011−4017

So, if the HPW12 loading is properly adjusted in order to prevent Keggin units from penetrating the interlayers of BN, the latter renders HPW12 more active than it is in its pure bulk-activated state. This ability to top the activity of the pure bulk-activated HPW12 is due to the fact that BN allows further increasing the Keggin units' dispersion compared to the pure bulk-activated HPW12 without weakening their protons' acid strength. It makes BN a truly suitable support, in contrast to the commonly used TiO_2, which, whatever the HPW12 loading, weakens the acid strength of the Keggin units' protons so much that the conversion per milligram of HPW12 (Figure 8b) does not even exceed a fifth of the value reached with the pure bulk-activated HPW12. Notice that the unsuitability of TiO_2 as a support for HPW12 in the methanol-to-DME reaction, and thus the need to find alternative supports such as the here revealed BN, had hitherto never been enlightened as teams have always been comparing the activities of TiO_2-supported HPW12 and pure HPW12 without having activated the latter's bulk, and thus by having underestimated the latter's activity and therefore overestimated the interest of TiO_2 (e.g., in ref 3).

4. CONCLUSIONS

In the present work, we highlight for the first time the interest of supporting HPW12 on hexagonal BN to get highly active catalysts in the gas phase methanol-to-DME reaction at 150 °C. As references, we use pure HPW12 in its most active state (namely after activation of its bulk thanks to an elsewhere recently reported procedure) and HPW12 supported on the commonly used TiO_2 support. HPW12 appears to interact with BN instead of forming independent aggregates, however by deviating from the tendency to form an ideal monolayer from the lowest loadings (unlike what is observed on TiO_2). As a consequence of the latter deviation, the BN-supported catalysts contain exclusively strong acid sites, namely as strong as within the pure HPW12. Then, as a consequence of both the only presence of strong acid sites and the absence of independent HPW12 aggregates, the BN-supported catalysts are all more active than their equivalent (in terms of % ML of HPW12) TiO_2-supported catalysts, which contain quasi-exclusively medium acid sites. Whatever the HPW12 loading, TiO_2-supported catalysts never show a methanol conversion that exceeds the fifth of the value reached with the pure bulk-activated HPW12. In opposition, BN is such a good support that, compared to the pure bulk-activated HPW12, there is even one BN-supported catalyst that wins the competition in terms of methanol conversion per milligram of HPW12: the one with 16% ML of HPW12 (showing 10.2% of conversion per milligram of HPW12 vs only 6.3% reached with the pure HPW12), which has the most accessible Keggin units.

■ ASSOCIATED CONTENT

Supporting Information

The Supporting Information is available free of charge on the ACS Publications website at DOI: 10.1021/acscatal.7b00808.

Nominal and real HPW12 loadings both in % ML and in weight % on both supports, N_2 physisorption isotherms of the pure supports, FT-IR spectra of the TiO_2-supported catalysts as well as of pure TiO_2 and pure BN, and NH_3-TPD profiles of the BN-supported catalysts with nominal loadings ≤40% ML (PDF)

■ AUTHOR INFORMATION

Corresponding Author

*E-mail: eric.gaigneaux@uclouvain.be.

ORCID

Josefine Schnee: 0000-0002-5260-8224

Notes

The authors declare no competing financial interest.

■ ACKNOWLEDGMENTS

The authors acknowledge the Université catholique de Louvain for the financial support and the combined teaching assistant−Ph.D. student position of J.S., as well as François Devred (Research Engineer at the Université catholique de Louvain, in the Institute of Condensed Matter and Nanosciences) for his useful technical advice regarding the use of the NH_3-TPD and XRD setups, and the *Communauté française de Belgique* for the financial support through the ARC program (15/20-069).

■ REFERENCES

(1) Kozhevnikov, I. V. *J. Mol. Catal. A: Chem.* **2007**, *262*, 86−92.
(2) Janik, M. J.; Campbell, K. A.; Bardin, B. B.; Davis, R. J.; Neurock, M. *Appl. Catal., A* **2003**, *256*, 51−68.
(3) Ladera, R. M.; Ojeda, M.; Fierro, J. L. G.; Rojas, S. *Catal. Sci. Technol.* **2015**, *5*, 484−491.
(4) Alharbi, W.; Kozhevnikova, E. F.; Kozhevnikov, I. V. *ACS Catal.* **2015**, *5*, 7186−7193.
(5) Fu, Y.; Hong, T.; Chen, J.; Auroux, A.; Shen, J. *Thermochim. Acta* **2005**, *434*, 22−26.
(6) Yaripour, F.; Baghaei, F.; Schmidt, I.; Perregaard, J. *Catal. Commun.* **2005**, *6*, 147−152.
(7) Ladera, R. M.; Fierro, J. L. G.; Ojeda, M.; Rojas, S. *J. Catal.* **2014**, *312*, 195−203.
(8) Popa, A.; Sasca, V.; Kiš, E. E.; Marinković-Nedučin, R.; Bokorov, M. T.; Halasz, J. *J. Optoelectron. Adv. Mater.* **2005**, *7*, 3169−3177.
(9) Schnee, J.; Gaigneaux, E. M. *Catal. Sci. Technol.* **2017**, *7*, 817−830.
(10) Golberg, D.; Bando, Y.; Huang, Y.; Terao, T.; Mitome, M.; Tang, C.; Zhi, C. *ACS Nano* **2010**, *4*, 2979−2993.
(11) Sugii, T.; Ohnishi, R.; Zhang, J.; Miyaji, A.; Kamiya, Y.; Okuhara, T. *Catal. Today* **2006**, *116*, 179−183.
(12) Aradi, E.; Naidoo, S. R.; Billing, D. G.; Wamwangi, D.; Motochi, I.; Derry, T. E. *Nucl. Instrum. Methods Phys. Res., Sect. B* **2014**, *331*, 140−143.
(13) Sakai, N.; Fujishima, A.; Watanabe, T.; Hashimoto, K. *J. Phys. Chem. B* **2003**, *107*, 1028−1035.
(14) Wattanakul, K.; Manuspiya, H.; Yanumet, N. *J. Appl. Polym. Sci.* **2011**, *119*, 3234−3243.
(15) Li, H.; Zeng, X. C. *ACS Nano* **2012**, *6*, 2401−2409.
(16) Raj, G.; Swalus, C.; Arendt, E.; Eloy, P.; Devillers, M.; Gaigneaux, E. M. *Beilstein J. Nanotechnol.* **2014**, *5*, 1749−59.
(17) Karimi, Z.; Mahjoub, A. R.; Harati, S. M. *Inorg. Chim. Acta* **2011**, *376*, 1−9.
(18) Kovtyukhova, N. I.; Wang, Y.; Lv, R.; Terrones, M.; Crespi, V. H.; Mallouk, T. E. *J. Am. Chem. Soc.* **2013**, *135*, 8372−8381.
(19) Ji, H.; Sun, J.; Wu, P.; Dai, B.; Chao, Y.; Zhang, M.; Jiang, W.; Zhu, W.; Li, H. *J. Mol. Catal. A: Chem.* **2016**, *423*, 207−215.
(20) Shen, L.; Feng, Y.; Yin, H.; Wang, A.; Yu, L.; Jiang, T.; Shen, Y.; Wu, Z. *J. Ind. Eng. Chem.* **2011**, *17*, 484−492.
(21) Shen, L.; Yin, H.; Wang, A.; Feng, Y.; Shen, Y.; Wu, Z.; Jiang, T. *Chem. Eng. J.* **2012**, *180*, 277−283.

DOI: 10.1021/acscatal.7b00808
ACS Catal. 2017, 7, 4011−4017